Seismic data reconstruction by inversion to common offset

Nizar Chemingui [†]

ExxonMobil Upstream Research Company, P.O Box 2189, Houston TX 77252

Biondo Biondi

Stanford Exploration Project, Mitchell Bldg., Department of Geophysics,

Stanford University, Stanford, CA 94305-2215

(October 3, 2001)

ABSTRACT

Preserving amplitude information when imaging 3-D multichannel seismic data is a challenging task. The imaging process can be described as seeking the inverse for a large matrix that relates the data to a reflectivity model. Due to the irregular coverage of 3-D surveys, the matrix is often ill-conditioned and its coefficients are badly scaled. We present a new approach for regularizing the coverage of 3-D surveys by partial imaging before migration. After regularization, 3-D data become better suited for prestack migration using either "true amplitude" Kirchhoff methods or wave extrapolation techniques.

Posing partial stacking before migration as an inverse problem, we develop a new optimization technique named "inversion to common offset" (ICO) that solves for optimal partial stacks from multi-fold 3-D data. The inversion approach takes advantage of the redundancy of information present in multichannel recording to recover densely and regularly sampled common-offset common-azimuth volumes. The reconstruction of each of these

[†]Formerly Stanford Exploration Project, Department of Geophysics, Stanford University, Stanford, CA 94305-2215

cubes combines data from multiple incomplete experiments over a common earth model to simulate the ideal data that would have been recorded from a single common-offset common-azimuth experiment. The method is based on the inversion of a partial prestack migration operator that maps seismic data from a given acquisition geometry to an arbitrary one. This data mapping operator is the azimuth moveout operator (AMO). The main advantage of ICO is that the AMO operator is compact and consequently cheaper to apply than other imaging operators, such as full 3-D prestack migration.

We present a cost-effective implementation of ICO based on a log-stretch transformation of the time axis. After this transformation, AMO becomes time invariant, so the inversion can be performed in the Fourier domain on each temporal-frequency slice independently. To accelerate the convergence of the iterative solution, we precondition the system of linear equations by two diagonal transformations that scale the rows and columns of the modeling operator. A stable solution is achieved by adding a penalty function that constrains the spatial variability of the model.

Results of applying ICO to a field 3-D land survey show that we can recover the high-frequency features of the reflectivity function from a severely undersampled data set obtained by decimating a densely sampled prestack data set. The images obtained by prestack migration after regularization are superior to those produced by direct migration of the decimated data.

INTRODUCTION

The growing need for detailed reservoir descriptions has led to the careful handling of amplitudes from 3-D reflection data. Therefore, imaging seismic data for amplitude interpretation

has found many applications in AVO analysis, fluid imaging, and reservoir monitoring. For that Kirchhoff techniques have been subject of extensive studies with asymptotic inverse theory applied to derive optimal weights for the Kirchhoff summation (Sullivan and Cohen, 1987; Bleistein, 1987; Hanitzsch et al., 1994). Recently Kirchhoff theory has been extended to take explicitly into account irregular data sampling and poor reflector illumination (Albertin et al., 1999; Bloor et al., 1999; Audebert, 2000; Rousseau et al., 2000; Jousset et al., 2000). These methods are promising for equalizing image amplitudes when the data are irregularly but adequately sampled. Their effectiveness to correct for amplitude and phase distortions when the data are undersampled is still uncertain.

We follow a different approach to imaging based on optimization theory and iterative inversion to handle incomplete and redundant seismic data. Instead of attempting derivation of an explicit inverse, the optimization approach iteratively solves for a model that best fits the recorded seismic data. The model can be a seismic image (Cole and Karrenbach, 1992; Schuster, 1993; Duquet et al., 1998; Nemeth et al., 1999), or a regularly sampled dataset that simulates an ideal acquisition geometry, such as zero-offset data (Ronen, 1987).

Iterative methods can be computationally expensive because they require several applications of an imaging operator and of its adjoint. Consequently, they are seldom employed in large scale seismic imaging. In particular, applying 3-D prestack migration as an iterative technique is still a huge computational task. To overcome these difficulties, we propose a new solution that generates high-quality prestack images while being orders of magnitude cheaper than iterative inversion of 3-D prestack migration. The method splits the imaging problem into two steps. The first step is data reduction and regularization by optimized partial imaging of normal moveout corrected data. The imaging operator that we invert is the azimuth moveout operator (AMO) introduced by Biondi and Chemingui (1994) and

Biondi et al. (1998). The inversion produces regularly sampled common-offset common-azimuth volumes, so we named this step inversion to common offset (ICO). The second step applies true-amplitude migration to the regularly sampled partial stacks. In this paper we focus on the development of ICO's methodology. The theory and practice of true-amplitude migration of regularly sampled data is beyond the scope of this work, and is amply discussed in the literature.

The splitting of the full prestack imaging process into the two steps of regularization followed by true amplitude migration is similar to the reconstruction approach presented by Duijndam et al. (2000). However, they use a simple Fourier interpolator to connect the irregularly sampled data to the data reconstructed on a regular grid. In our approach, we use a seismic imaging operator (AMO) to map between the two data spaces, and thus the inversion fully exploits the inherent correlation between seismic traces from the same reflection survey.

The first section of our paper presents the theory and the formulation of the least-squares solution for multichannel seismic data. The second section addresses practical issues of the implementation of the inversion, namely, cost efficiency in the log-stretch Fourier domain, proper preconditioning, and regularization of the iterative solution. Finally, the last section of the chapter demonstrates the application of the technique to the imaging of a 3-D land survey. It illustrates an example of applying ICO to reduce the size of the survey and to improve the quality of the image by regularizing the geometry of the data before migration.

INVERSION TO COMMON OFFSET

The offset dimension adds important aspects to reflection seismology. Mainly, it provides robust analysis of the velocity of seismic waves and enables enhancement of signal-to-noise ratio by stacking. We use the offset and azimuth dimensions to pose imaging as an optimization process that recovers the best migrated images from multi-shot and multi-trace seismic data. We exploit Kirchhoff-style implementations of imaging operators to better accommodate any type of irregular geometry. The implementation of integrals as discrete summation reduces to a matrix-vector multiplication. The linear operation transforms a space to another space (e.g., a data space $\mathbf{D}$ to a model space $\mathbf{M}$). These spaces are simply represented by vectors whose components are packed with numbers. The relation between data and model is then given by the linear system of equations:

$$\mathbf{d} = \mathbf{L}\mathbf{m}. \tag{1}$$

Equation (1) represents a forward modeling relation, whereas the goal of imaging is to perform the inverse of these calculations, i.e., to find models from the data. Mathematically, this is equivalent to estimating the inverse of $\mathbf{L}$.

Given the nature of multi-channel recording and the design of 3-D surveys, the number of data traces is usually different from the number of model traces. Most commonly, the number of observations is larger than the number of model parameters. One way to solve such a system of inconsistent equations is to look for a solution that minimizes the average error in the set of equations. This minimization can be done in a least-squares sense where the norm $\|\mathbf{L}\mathbf{m} - \mathbf{d}\|_\mathbf{2}$ is minimized. The choice of $\mathbf{m}$ that reduces this error to a minimum is the least-squares solution

$$\mathbf{m} = (\mathbf{L^T}\mathbf{L})^{-\mathbf{1}}\mathbf{L^T}\mathbf{d}. \tag{2}$$

Considering multiple records at every CMP bin to present redundant information, the inversion for a reflectivity model from multi-offset seismic data is generally an over-determined problem. However, in many geophysical applications the size of the model space is not fixed but rather determined according to a desired resolution, computational costs and anti-aliasing criteria. Moreover, whenever gaps in seismic coverage occur, the problem becomes locally under-determined. Therefore, the linear system to be solved is often ill-conditioned and care must be taken when approximating the inverse of $\mathbf{L}$.

The use of inverse theory requires the choice of a forward modeling operator. We define processing as the inverse of modeling irregularly sampled data from a regularly sampled model (Ronen, 1994; Chemingui and Biondi, 1997). For practical reasons, mainly cost-efficiency of the inversion on 3-D data, we address the case of partial stacking by AMO. The inverse of AMO-stacking is AMO modeling from a regularly sampled common-azimuth and common-offset volume into irregularly sampled data with a range of offsets and azimuths. The next section discusses the azimuth moveout operator and its integral implementation in the X-T space.

THE AZIMUTH MOVEOUT OPERATOR (AMO)

This section is a brief review of the azimuth moveout operator. AMO is a partial prestack imaging operator that rotates the azimuth and modifies the offset of 3-D prestack data. It moves events across midpoints according to their dip and therefore preserves all the high frequency components in the data during partial stacking. As in DMO processing (Deregowski and Rocca, 1981; Hale, 1984), the first-order effects of velocity variation are removed by applying a normal moveout correction (NMO) to the data prior to AMO.

The impulse response of AMO is described by a saddle in the output midpoint domain. The shape of the saddle depends on the offset vector of the input data $\mathbf{h}_1 = h_1 \cos\theta_1 \mathbf{x} + h_1 \sin\theta_1 \mathbf{y} = h_1(\cos\theta_1, \sin\theta_1)$ and on the output offset vector $\mathbf{h}_2 = h_2(\cos\theta_2, \sin\theta_2)$, where the unit vectors $\mathbf{x}$ and $\mathbf{y}$ point respectively in the in-line direction and the cross-line direction. The analytical expression of the AMO saddle, as given by Biondi et al. (1998), is,

$$t_2\left(\mathbf{\Delta m}, \mathbf{h}_1, \mathbf{h}_2, t_1\right) = t_1 \frac{h_2}{h_1} \sqrt{\frac{h_1^2 \sin^2(\theta_1 - \theta_2) - \Delta m^2 \sin^2(\theta_2 - \Delta\varphi)}{h_2^2 \sin^2(\theta_1 - \theta_2) - \Delta m^2 \sin^2(\theta_1 - \Delta\varphi)}}. \tag{3}$$

The traveltimes t_1 and t_2 are the traveltime of the input data after normal moveout correction and the traveltime of the results before inverse NMO. The midpoint vector $\mathbf{\Delta m} = \Delta m(\cos\Delta\varphi, \sin\Delta\varphi)$ is the difference between the input and output midpoint location vectors.

Detailed derivations for a true-amplitude function for the AMO operator were presented by Chemingui and Biondi (1995). These weights are given by the following expression:

$$A\left(\mathbf{\Delta m}, \mathbf{h}_1, \mathbf{h}_2, t_2\right) \approx \frac{|\omega_2|\, t_2}{2\,\pi\, h_1 h_2\, \sin\Delta\theta} \frac{1 + \frac{\Delta m^2 \sin^2(\theta_2 - \Delta\varphi)}{h_1^2 \sin^2\Delta\theta}}{\left(1 - \frac{\Delta m^2 \sin^2(\theta_2 - \Delta\varphi)}{h_1^2 \sin^2\Delta\theta}\right)\left(1 - \frac{\Delta m^2 \sin^2(\theta_1 - \Delta\varphi)}{h_2^2 \sin^2\Delta\theta}\right)}. \tag{4}$$

The frequency term $|\omega_2|$ enters as a multiplicative factor in the expression for AMO amplitudes. This term can be applied to the output data in the time domain by chaining a causal half-differentiator with an anti-causal half-differentiator.

The domain of influence of the AMO operator is defined by the the region of validity of expression (1). For given $\mathbf{h_1}$ and $\mathbf{h_2}$, the bounds for the AMO aperture are functions of the input traveltime and the minimum velocity V_{min} (Biondi et al., 1998).

For small azimuthal rotations, the saddle describing the AMO impulse response has a

strong curvature that requires special handling of operator antialiasing. The trick is to perform the spatial integration in a transformed coordinate system where the AMO surface becomes invariant with respect to the amount of azimuth rotation and offset continuation. The appropriate midpoint-coordinate transformation is described by the following chain of transformations (Fomel and Biondi, 1992):

$$\begin{bmatrix} \xi_1 \\ \xi_2 \end{bmatrix} = \begin{bmatrix} \frac{1}{h_2 \sin \Delta\theta} & 0 \\ 0 & \frac{1}{h_1 \sin \Delta\theta} \end{bmatrix} \begin{bmatrix} -\sin\theta_1 & \cos\theta_1 \\ -\sin\theta_2 & \cos\theta_2 \end{bmatrix} \begin{bmatrix} \Delta m_x \\ \Delta m_y \end{bmatrix} , \tag{5}$$

where ξ_1, and ξ_2 are the transformed midpoint coordinates.

In this coordinate system, the kinematics of AMO are described by the following simple relationship between the input time t_1 and the output time t_2

$$t_2(\xi_1, \xi_2) = t_1 \sqrt{\frac{1-{\xi_2}^2}{1-{\xi_1}^2}} , \tag{6}$$

and the amplitudes are described by the following equation

$$A(\xi_1, \xi_2) = \frac{t_2 |\omega_2|}{2\pi} \frac{\left(1+{\xi_1}^2\right)}{\left(1-{\xi_1}^2\right)\left(1-{\xi_2}^2\right)} . \tag{7}$$

which takes into account the Jacobian factor introduced by the coordinate transformation.

Figure 1 shows the surface of the AMO impulse response for three given spikes at times $t_1 = .75, 1.$ and 1.25 s when h_1 is equal to 800 m, h_2 is equal to 1 km, θ_1 is equal to zero degrees, θ_2 is equal to 25 degrees and V_{min} is equal to 1.5 km/sec. The AMO saddle is very compact and shrinks with increasing recording time.

Figure 2 provides an intuitive understanding of the computational advantage of AMO compared with full 3-D prestack migration. It shows the impulse response of prestack migration for the same input spikes and the same geometry used for the AMO impulse responses shown in Figure 1. While the aperture of AMO is very compact and decreases

with time, the migration aperture is quite large and increases with depth. At a depth of 1.5 km it is already bigger than the size of the display model (4 km^2). This difference in operator aperture makes the cost of AMO small compared to the cost of full 3-D prestack migration.

PRACTICAL IMPLEMENTATION OF ICO

Inversion of 3-D multichannel seismic data using wave-equation techniques is generally cost prohibitive. The main reason for the high cost is the size of the prestack data and the time and space-variability of wave equation processes. The advantages of ICO is that the modeling operator, AMO, is very compact and reasonably inexpensive to apply, and that ICO is also velocity independent since it is applied to normal-moveout corrected data. In the following sections, we present a cost-effective implementation of ICO on 3-D data.

Log-stretch Fourier transformation

Several authors (Bolondi et al., 1982; Biondi and Ronen, 1986; Bale and Jakubowicz, 1987; Notfors and Godfrey, 1987; Liner, 1990) described a logarithmic stretching of the time axis to convert an imaging operator (e.g. DMO) that is non-stationary along the time axis into a time-stationary operator, which can then be efficiently applied in the Fourier domain.

The log-stretch transform makes AMO a time-invariant operator, which means it only depends on the difference between the input and output time. Detailed derivations for AMO in the log-stretch domain are presented in the appendix. After log-stretching, Fourier transformation of the time axis makes each frequency inversion completely independent, so one needs only to solve many small decoupled systems of equations instead of solving one

single huge system. In practice, several frequency bands from a useful bandwidth of the data can be processed in parallel.

Iterative solution for the pseudo-inverse

For each frequency component (or bandwidth) the system of linear equations to be solved is still very large and one has to resort to iterative methods. This solves a large set of simultaneous equations without the need to write down the matrix of coefficients. We use an iterative scheme based on the conjugate gradient solver. The algorithm generates a sequence of approximate solutions whose computations each involve the application of the adjoint followed by the forward operator. Both operations are AMO transformations and their computation is therefore reasonably cheap.

Preconditioning Kirchhoff operators

The convergence rate of the conjugate gradient algorithm depends on the condition number of the matrix to be inverted. For ill-conditioned matrices a preconditioner is often necessary and its design depends directly on the structure of the matrix. In relation (1), the number of equations is the number of traces in the input data and the number of unknowns is the number of output traces or bins. Since $\mathbf{L}$ is a Kirchhoff matrix, each row of $\mathbf{L}$ corresponds to a summation surface and each column corresponds to an impulse response. Due to irregular sampling, the rows and columns of $\mathbf{L}$ are badly scaled. To balance the coefficients of the matrix we apply a diagonal transformation to normalize its rows and columns. This involves pre- and post-multiplying the operator $\mathbf{L}$ by diagonal matrices $\mathbf{R}^{-1}$ and $\mathbf{c}^{-1}$ whose entries are the inverses of the sum of the rows or columns of $\mathbf{L}$. The sums are always positive

since Kirchhoff operators are associated with matrices that contain no negative elements. By scaling the Kirchhoff matrix, the operator $\mathbf{L}$ is normalized by its response to an input vector with all components equal to one. This is equivalent to calibrating the final image by a flat event.

The proposed preconditioning transformation recasts the original inversion relation (1) into the following

$$\mathbf{R}^{-n}\mathbf{d} = \mathbf{R}^{-n}\mathbf{L}\mathbf{C}^{n-1}\mathbf{x}. \tag{8}$$

where $0 \leq n \leq 1$.

The sums of the elements from each row of $\mathbf{L}$ are along the diagonal of $\mathbf{R}$ and from each column are along the diagonal of $\mathbf{C}$.

When $n = 0$, equation (8) reduces to the familiar case of column scaling. The preconditioning operator introduces a new model $\mathbf{x}$ given by

$$\mathbf{x} = \mathbf{C}\mathbf{m} \tag{9}$$

and the original inversion relation (1) is reformulated as:

$$\mathbf{d} = \mathbf{L}\mathbf{C}^{-1}\mathbf{x}. \tag{10}$$

After solving for $\mathbf{x}$ we easily compute $\mathbf{m} = \mathbf{C}^{-1}\mathbf{x}$.

Given that each column of $\mathbf{L}$ corresponds to an output bin, $\mathbf{C}^{-1}$ is normalization of the model by the coverage after AMO.

The case of $n = 1$ reduces to row scaling in the data space and solving the system:

$$\mathbf{R}^{-1}\mathbf{d} = \mathbf{R}^{-1}\mathbf{L}\mathbf{m} \tag{11}$$

$\mathbf{R}^{-1}$ is normalization of the data by the coverage before AMO. This data-space preconditioner can be interpreted as an approximation to a "data covariance" operator that is

used to express the reliability and the correlation of the data measurements. In iteratively re-weighted least squares, it approximates a data variance measure that can be estimated from the current residual.

The diagonal transformation (8) has proved to be a suitable preconditioner for the linear system. A good solution was obtained after 5 to 8 iterations of a conjugate gradient solver using a value of $n = 1/2$. An optimal value of n should depend on whether the system is mostly over-determined or under-determined.

Regularization of the inversion

In order to compute stable solutions to ill-conditioned systems it is often necessary to apply regularization methods. Claerbout (1998) writes: " In geophysical inversion we generally have two goals, the first being data "fitting" and the second being the "styling" of the model space". One way to achieve these objectives is to augment the problem with a second regression that adds assumptions about the model. We now seek a solution to the system of regressions:

$$0 \quad \approx \quad \mathbf{r}_d \quad = \quad \mathbf{L}\,\mathbf{m} \;-\; \mathbf{d} \tag{12}$$

$$0 \quad \approx \quad \mathbf{r}_m \quad = \quad \lambda\,\mathbf{P}\,\mathbf{m} \tag{13}$$

Where $\mathbf{r}_d$ is the data residual, $\mathbf{r}_m$ is the model residual and $\mathbf{P}$ is a "model-styling" operator. To impose a smoothness constraint on the solution, we chose $\mathbf{P}$ to be the Laplacian operator, which represents spatial differentiation in the midpoint-space. Setting the penalty operator, $\mathbf{P}$, to be the identity matrix reduces to the standard Tikhonov regularization (Tikhonov and Arsenin, 1977). The parameter λ controls the smoothness of the solution and is a function of the smallest resolved singular value of $\mathbf{L}$.

APPLICATION TO 3-D FIELD DATA

This section presents the results of applying ICO to a 3-D land survey recorded in the Shorncliff region of Canada. The quality of the data is very high as shown by the NMO stack in Figure 3. The dominant geology of the area is flat. One of the objective targets is a shallow (approximately 0.71 seconds) fluvial deposit system marked by a buried meandering channel. The shallow depth of this target zone makes it sensitive to acquisition geometries. Previous studies of the data set focused on DMO processing and inversion to zero offset (Ronen and Goodway, 1998). In our application, we address problems related to prestack depth imaging and the effects of irregular sampling on the image quality.

The survey was designed with the aim of obtaining a high fold coverage for a good quality final stack. The image from the densely-sampled survey can then be used to assess the quality of images obtained by simulating more economic acquisition geometries. The data were acquired using a cross-spread geometry, which provides a wide range of azimuths at near offsets but a narrower range at far offsets (Figure 4). The full survey consists of about 1.4 million traces with maximum offset of 3 km. The shot and receiver spacing is 70 meters for a nominal CMP spacing of 35 meters in both in-line and cross-line directions.

Since the original data set was densely sampled, we decimated the survey to create a sparse geometry that results in aliasing problems. The shot lines from the densely-sampled survey are spaced at 140 meters, whereas in the decimated experiment they alternate between 280 and 420 m for an average spacing of 350 m. We also extracted every fifth receiver line to simulate a cross-spread grid with 350 m line-spacing as shown in Figure 5. The 3-D subset used in our tests consisted of 13,100 traces whose source-receiver azimuth is between -60^o and 60^o with an absolute-offset range from 400 to 1,000 meters. We partitioned both

the offset and azimuth axes to simulate a case in which the reflection amplitude dependency on both azimuth and offset is of interest.

Figure 6 shows the fold distribution for the subset binned at the survey nominal CMP spacing of 35 m. Variations in coverage between different bins range from 0 to a maximum of 7. If not properly accounted for, these variations in fold can distort the quality of the final image. In comparison, Figure 7 represents a fold chart for the same offset and azimuth range from the original survey. The densely-sampled subset contains 148,000 traces, and therefore, is 13 times larger than the decimated survey.

Data regularization

To regularize the coverage of the coarsely-sampled subset, we applied the data reconstruction solution, namely AMO and ICO, to recover a regularly- sampled common-azimuth common-offset volume. The model is sampled at 17.5 m spacing with zero effective azimuth and 700 m constant offset. The top two panels from Figures 8 and 9 show the effects of the decimation on the input data. As expected, flat events were not destroyed by simple NMO binning. However, due to the low fold and the rapidly varying coverage between CMP bins, the signal to noise ratio is not homogeneous across the section. With normalized AMO (one iteration of ICO, calibrated by a flat-event response), amplitudes are still distorted and aliasing noise dominates the seismic sections. The result of regularized ICO with row and column scaling, after 7 iterations, is substantially better than calibrated AMO. Amplitudes along the flat reflectors are better equalized and aliasing noise is mostly eliminated.

Migration after regularization

The next step after regularizing the coverage of the 3-D subset is to apply 3-D migration to the partial stack. Although at this stage any wave-extrapolation technique can be applied to the regularly sampled subset, we chose Kirchhoff migration for consistency in comparing the results of imaging before and after regularization. Figure 10 shows a depth slice at 910 m where differences are most noticeable between the results. The migration of the original densely-sampled survey indicates a complex morphology of a meandering river system marked by ramification of the major channel. The image obtained by migrating the irregularly sampled subset is very noisy and distorted by strong artifacts that make the interpretation of the channels difficult. The result of migrating the AMO stack displays poor resolution and the channels are also unresolved. In contrast, migration after reconstruction with ICO unveiled the details of the channels and produced a good image comparable in resolution to the benchmark image from the densely-sampled survey. The sharpness of the image is attributed to the proper imaging of the diffractions from the edges of the levees and possible barrier islands in the river deposit system. While these diffractions were not properly reconstructed by partial stacking of the coarsely-sampled data when applying AMO, they were nicely preserved for imaging after optimized reconstruction by ICO.

CONCLUSIONS

We have presented a new approach for imaging irregularly sampled 3-D prestack data. The method poses partial stacking with AMO as an optimization process to reduce the size of prestack data and regularize its coverage before migration. The new inversion, named ICO, is applied to normal-moveout corrected data. It enables prestack analysis of the reflectivity

function since the output models are partial stacks at non-zero offset. The partial stacks can be migrated separately and either stacked together to form the final image, or individually analyzed for amplitude and velocity variations.

We have presented a cost effective implementation of ICO in the log-stretch Fourier domain with proper preconditioning and regularization of the inversion for iterative solvers. Results of applying ICO to a land 3-D survey showed that regularizing the coverage before imaging helps preserve the amplitude information and the high frequency components of the reflectivity function. Furthermore, ICO provides a promising approach for reducing the costs of 3-D acquisition.

ACKNOWLEDGMENTS

We thank PanCanadian Petroleum and in particular Bill Goodway for providing us with the 3-D dataset used for our tests. We also thank the sponsors of the Stanford Exploration Project for their financial support and ExxonMobil Upstream Research Company for permitting the publication of this work.

Paul Fowler and Craig Artley provided thorough review of the original manuscript and helped improve the quality of the exposition.

REFERENCES

Albertin, U., Jaramillo, H., Yingst, D., Bloor, R., Chang, W., Beasley, C., and Mobley, E., 1999, Aspects of true amplitude migration: 69th Annual Internat. Mtg., Soc. Expl. Geophys., Expanded Abstracts, 1358–1361.

Audebert, F., 2000, Restored amplitudes AVA-gathers in the multi-angle domain: 62nd Mtg. Eur. Assoc. Expl Geophys., Abstracts, P–142.

Bale, R., and Jakubowicz, H., 1987, Post-stack prestack migration: 57th Annual Internat. Mtg., Soc. Expl. Geophys., Expanded Abstracts, 714–717.

Biondi, B., and Chemingui, N., 1994, Transformation of 3-D prestack data by Azimuth Moveout (AMO): 64th Ann. Internat. Meeting, Soc. Expl. Geophys., Expanded Abstracts, 1541–1544.

Biondi, B., and Ronen, S., 1986, Shot profile dip moveout using log-stretch transform: 56th Annual Internat. Mtg., Soc. Expl. Geophys., Expanded Abstracts, 431–434.

Biondi, B., Fomel, S., and Chemingui, N., 1998, Azimuth moveout for 3-D prestack imaging: Geophysics, **63**, no. 2, 574–588.

Bleistein, N., 1987, On the imaging of reflectors in the earth: Geophysics, **52**, no. 7, 931–942.

Bloor, R., Albertin, U., Jaramillo, H., and Yingst, D., 1999, Equalised prestack depth migration: 69th Annual Internat. Mtg., Soc. Expl. Geophys., Expanded Abstracts, 1362–1365.

Bolondi, G., Loinger, E., and Rocca, F., 1982, Offset continuation of seismic sections : Geophys. Prosp., **30**, no.6, 813–828.

Chemingui, N., and Biondi, B., 1995, Amplitude preserving azimuth moveout: 65th Annual Internat. Mtg., Soc. Expl. Geophys., Expanded Abstracts, 1453–1456.

Chemingui, N., and Biondi, B., 1997, Equalization of irregular data by iterative inversion: 67th Annual Internat. Mtg., Soc. Expl. Geophys., Expanded Abstracts, 1115–1118.

Claerbout, J., 1998, Geophysical estimation by example: Environmental soundings image enhancement: http://sepwww.stanford.edu/sep/prof/.

Cole, S., and Karrenbach, M., 1992, Least-squares Kirchhoff migration: Stanford Exploration Project, SEP-Report 75, 101–110.

Deregowski, S. M., and Rocca, F., 1981, Geometrical optics and wave theory of constant offset sections in layered media: Geophys. Prosp., **29**, no. 3, 374–406.

Duijndam, A. J. W., Volker, A. W. F., and Zwartjes, P. M., 2000, Reconstruction as efficient alternative for least squares migration: 70th Ann. Internat. Meeting, Soc. Expl. Geophys., Expanded Abstracts, 1012–1015.

Duquet, B., Marfurt, K., and Dellinger, J., 1998, Efficient estimates of subsurface illumination for Kirchhoff prestack depth migration: 68th Ann. Internat. Meeting, Soc. Expl. Geophys., Expanded Abstracts, 1541–1544.

Fomel, S., and Biondi, B., 1992, Azimuth moveout: The operator parameterization and antialiasing: Stanford Exploration Project, SEP-Report 89, 89–107.

Hale, D., 1984, Dip-moveout by Fourier transform: Geophysics, **49**, no. 6, 741–757.

Hanitzsch, C., Schleicher, J., and Hubral, P., 1994, True-amplitude migration of 2D synthetic data: Geophys. Prosp., **42**, 445–462.

Jousset, P., Thierry, P., and Lambare, G., 2000, Improvement of 3D migration/inversion by reducing acquisition footprints: 62nd Mtg. Eur. Assoc. Expl Geophys., Abstracts, C–53.

Liner, C. L., 1990, General Theory and Comparative Anatomy of Dip Moveout: Geophysics, **55**, no.5, 595–607.

Nemeth, T., Wu, C., and Schuster, G. T., 1999, Least-squares migration of incomplete reflection data: Geophysics, **64**, no. 1, 208–221.

Notfors, C. D., and Godfrey, R. J., 1987, Dip moveout in the frequency-wavenumber domain (short note): Geophysics, **52**, no. 12, 1718–1721.

Ronen, S., and Goodway, W., 1998, Coverage and binning issues for marine seismic surveys: The Leading Edge, **17**, no. 11, 1600–1605.

Ronen, S., 1987, Wave-equation trace interpolation: Geophysics, **52**, no. 7, 973–984.

Ronen, S., 1994, Handling irregular geometry: Equalized DMO and beyond: 64th Ann. Internat. Meeting, Soc. Expl. Geophys., Expanded Abstracts, 1545–1548.

Rousseau, V., Nicoletis, L., Svay-Lucas, J., and Rakotoarisoa, H., 2000, 3D true amplitude migration by regularisation in angle domain: 62nd Mtg. Eur. Assoc. Expl Geophys., Abstracts, B–13.

Schuster, G., 1993, Least squares crosswell migration: 64th Ann. Internat. Meeting, Soc. Expl. Geophys., Expanded Abstracts, 110–113.

Sullivan, M. F., and Cohen, J. K., 1987, Prestack Kirchhoff inversion of common-offset data: Geophysics, **52**, no. 6, 745–754.

Tikhonov, A. N., and Arsenin, V. Y., 1977, solution of ill-posed problems: John Wiley and Sons.

APPENDIX

LOG-STRETCH AMO

The AMO operator as expressed in equation (6) is space and time-variant. Fortunately, after a logarithmic transformation of the time axis, AMO becomes time-invariant and therefore, can be applied efficiently in the Fourier domain.

The log-stretch transform uses the following change of variables:

$$t_1 = t_c \exp\left(\frac{\tau_1}{t_c}\right) \tag{A-1}$$

$$t_2 = t_c \exp\left(\frac{\tau_2}{t_c}\right) \tag{A-2}$$

$$\omega_2 = \Phi_2 \exp\left(-\frac{\tau_2}{t_c}\right) \tag{A-3}$$

where τ_1 and τ_2 are the log-stretched input and output traveltimes, Φ is the frequency dual of the log-stretched time axis, and t_c is a time constant that can be set for convenience to the smallest (non-zero) time of interest. With these changes of variables and after stretching, equation (6) of the main text becomes

$$\tau_2\left(\xi_1, \xi_2\right) = \tau_1 + t_c \log\left(\sqrt{\frac{1-{\xi_2}^2}{1-{\xi_1}^2}}\right). \tag{A-4}$$

The new operator is now time invariant since it only depends on the difference between the input and output traveltimes τ_1 and τ_2.

Substituting for ω and t_2 in equation (7), the amplitude weights for AMO in the new coordinate system are then given by

$$A\left(\xi_1, \xi_2\right) = \frac{t_c\left|\Phi_2\right|}{2\pi} \frac{\left(1+{\xi_1}^2\right)}{\left(1-{\xi_1}^2\right)\left(1-{\xi_2}^2\right)}. \tag{A-5}$$

which is now independent of time and hence convenient to apply in the Fourier domain.

To avoid operator aliasing, one should limit the maximum frequency according to the time dip of the operator which can be computed analytically according to

$$\frac{\partial \tau_2}{\partial \xi_1} = t_c \frac{\xi_1}{1 - {\xi_1}^2} \,, \tag{A-6}$$

$$\frac{\partial \tau_2}{\partial \xi_2} = -t_c \frac{\xi_2}{1 - {\xi_2}^2} \,. \tag{A-7}$$

Limiting the maximum frequency reduces the aperture of the operator and hence the costs of applying AMO.

Finally, to avoid truncation artifacts, a tapering function should be applied to the edges of the operator aperture.

LIST OF FIGURES

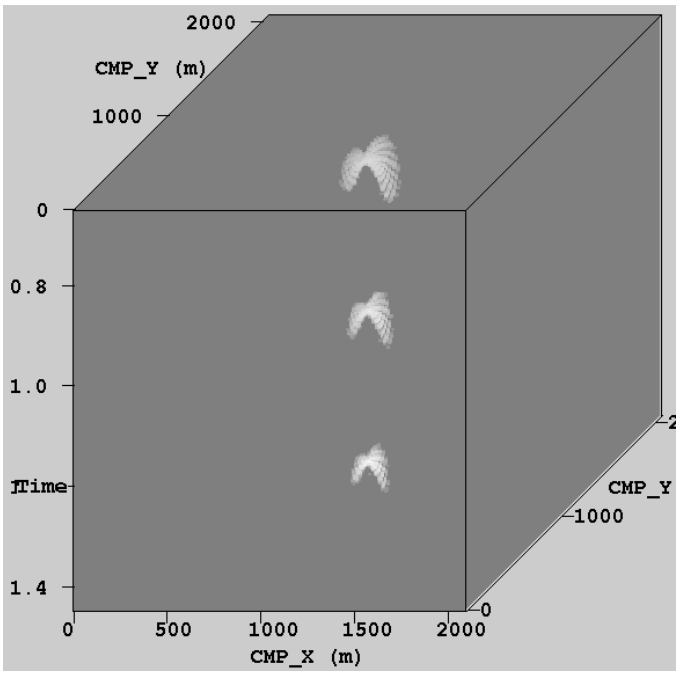
2000
CMP_Y (m)
1000
0
0.8
1.0
Time
1.4
0
500
1000
1500
2000
CMP_X (m)
CMP_Y
1000
0

Figure 1.

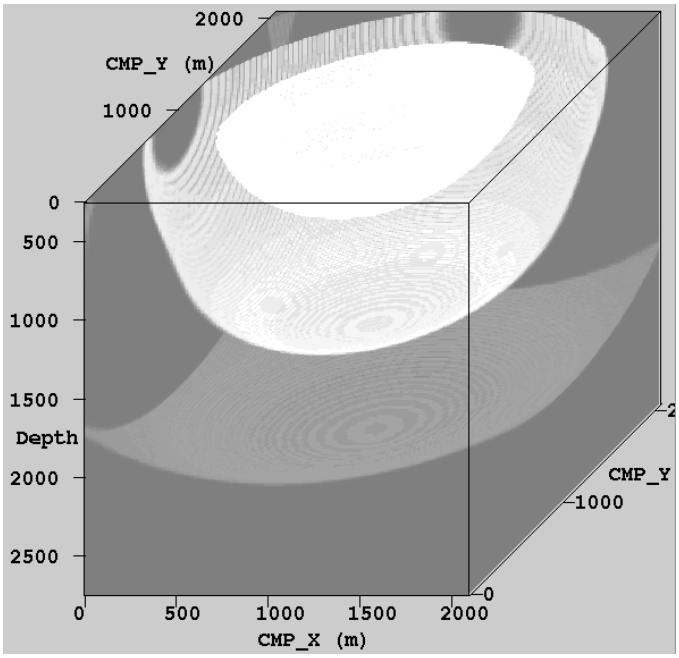
2000
CMP_Y (m)
1000
0
500
1000
1500
Depth
2000
2500
0
500
1000
1500
2000
CMP_X (m)
CMP_Y
1000
0

Figure 2.

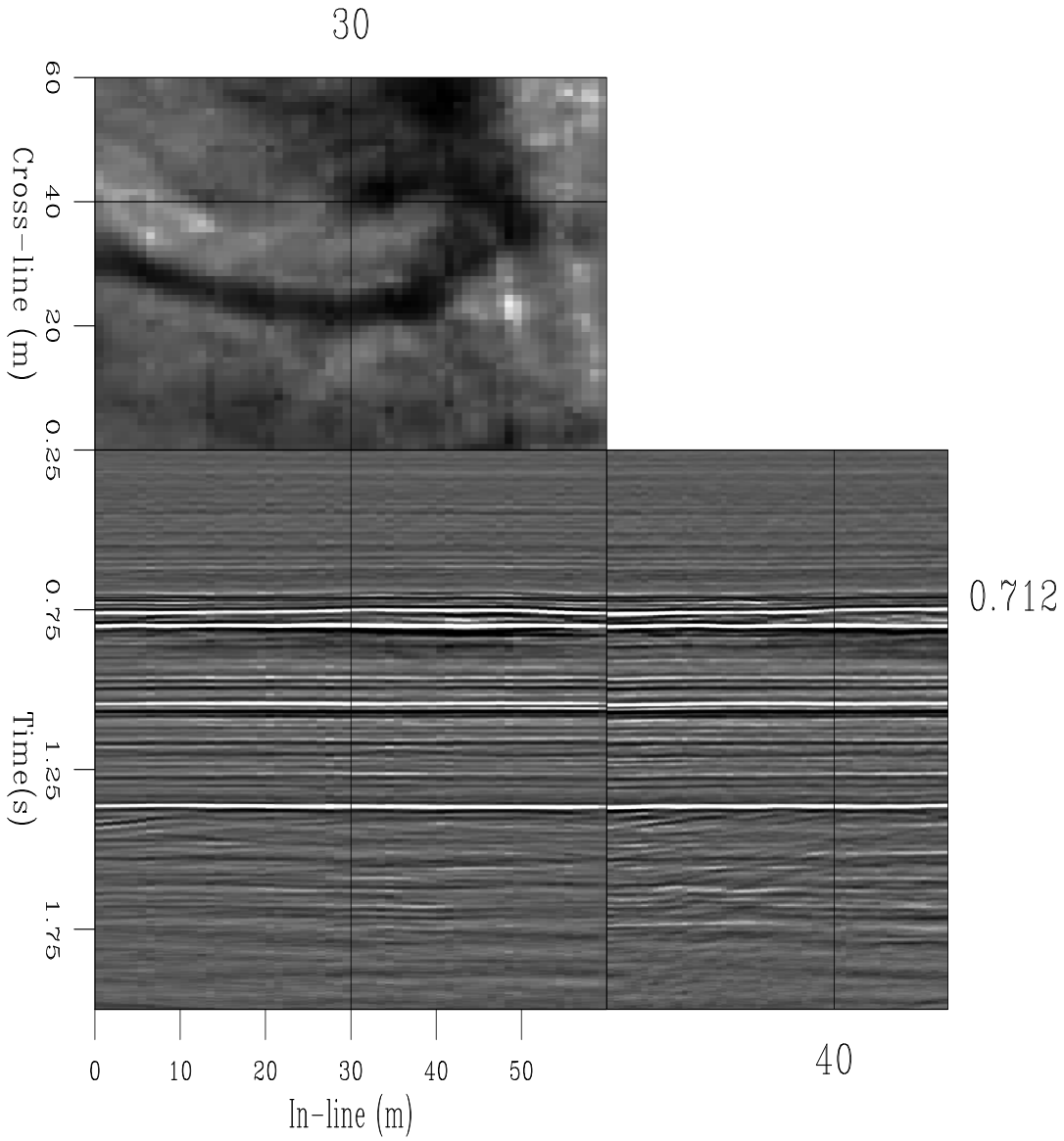
30
60
40
20
Cross−line (m)
0.25
0.75
1.25
1.75
Time(s)
0.712
0
10
20
30
40
50
40
In−line (m)

Figure 3.

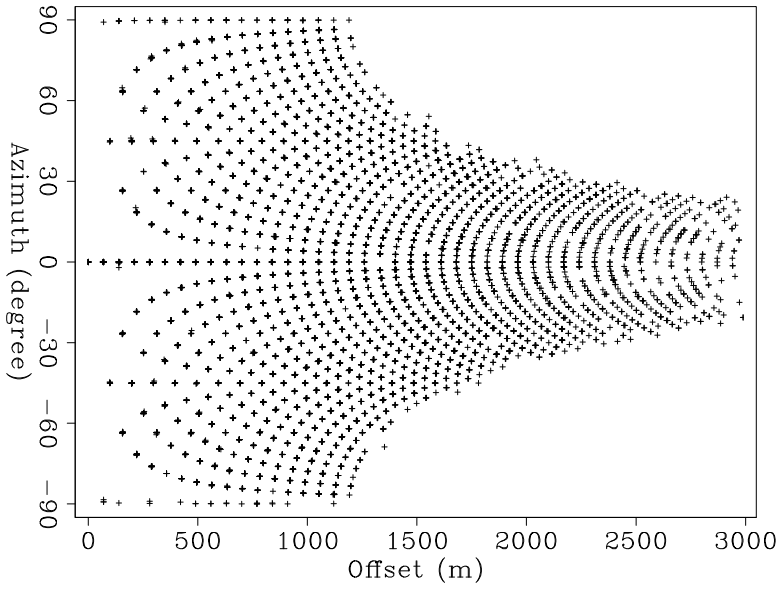
Azimuth (degree)
90
60
30
0
−30
−60
−90
0
500
1000
1500
2000
2500
3000
Offset (m)

Figure 4.

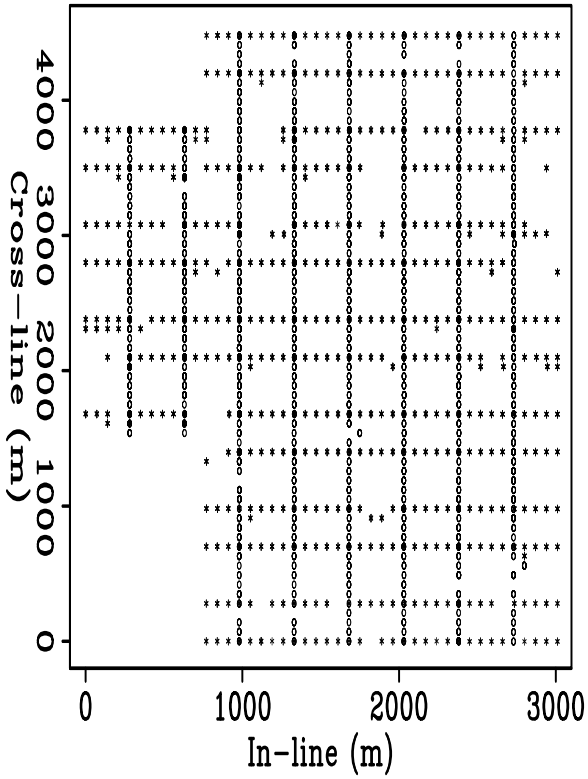

Figure 5.

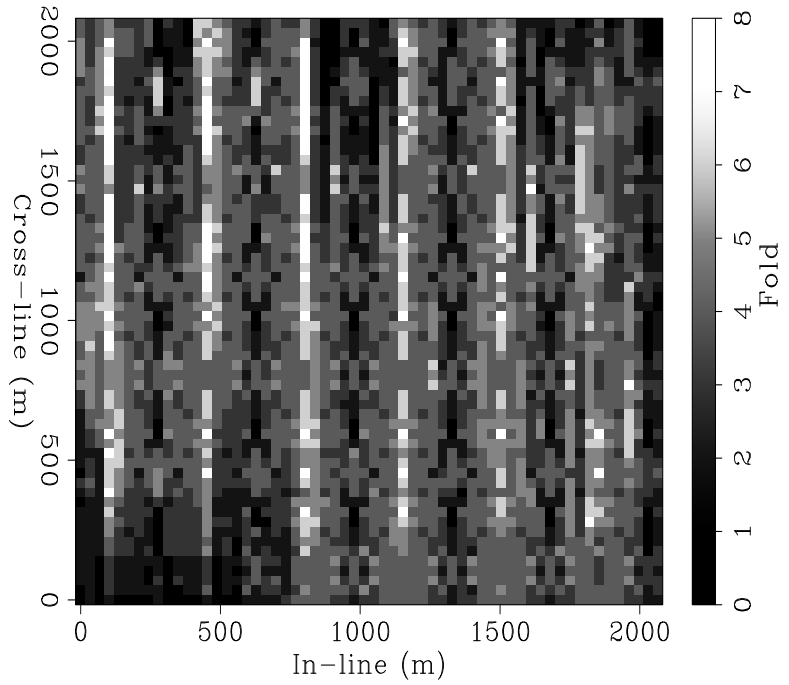
Cross−line (m)
0
500
1000
1500
2000
In−line (m)
0
500
1000
1500
2000
Fold
0
1
2
3
4
5
6
7
8

Figure 6.

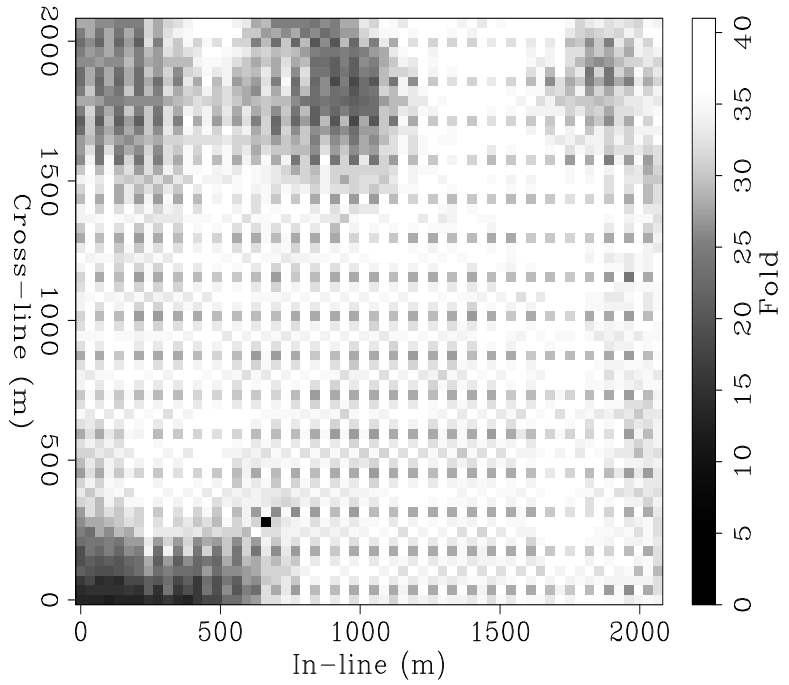
Cross−line (m)
0
500
1000
1500
2000
In−line (m)
0
500
1000
1500
2000
Fold
0
5
10
15
20
25
30
35
40

Figure 7.

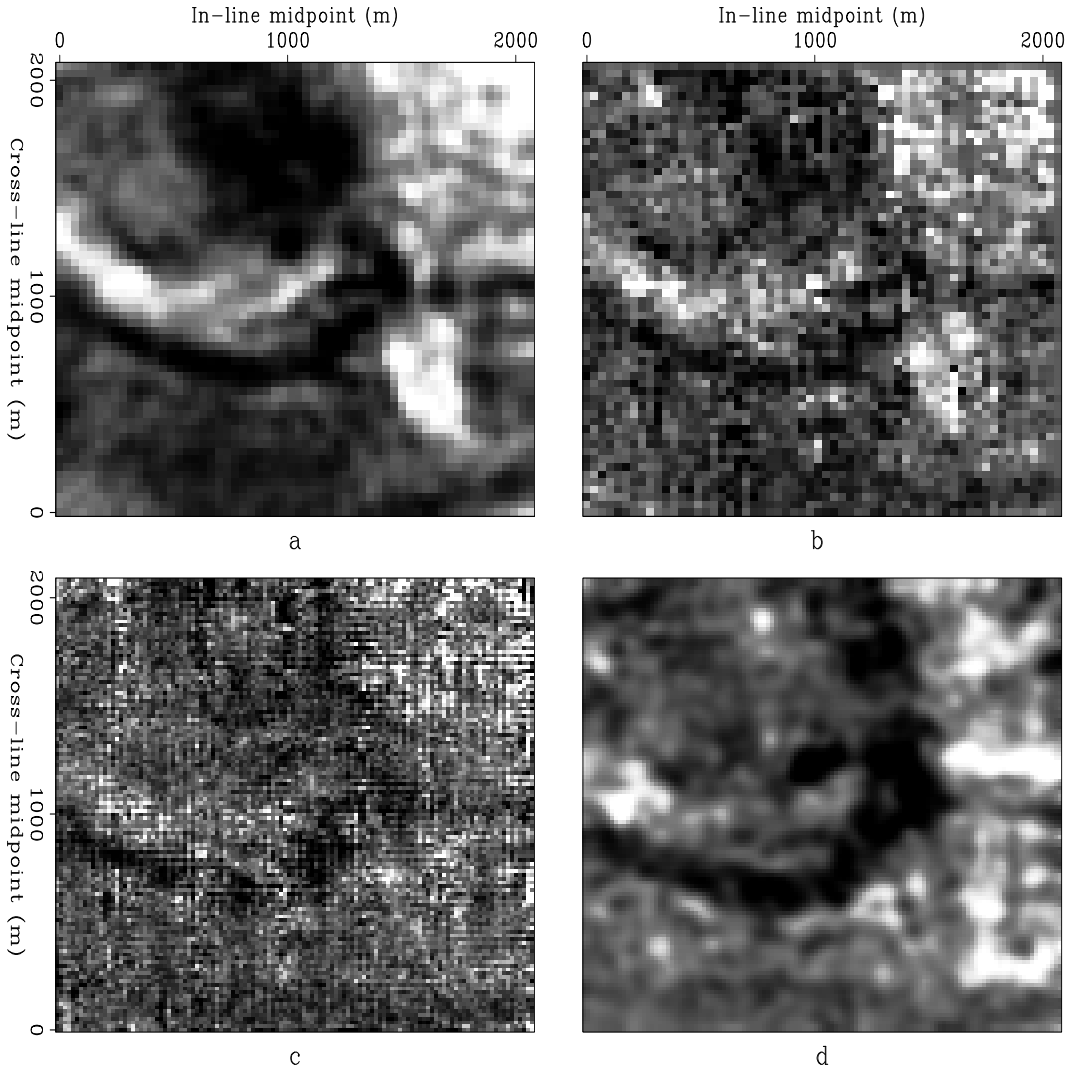
In−line midpoint (m)
0
1000
2000
Cross−line midpoint (m)
0
1000
2000
a
b
c
d

Figure 8.

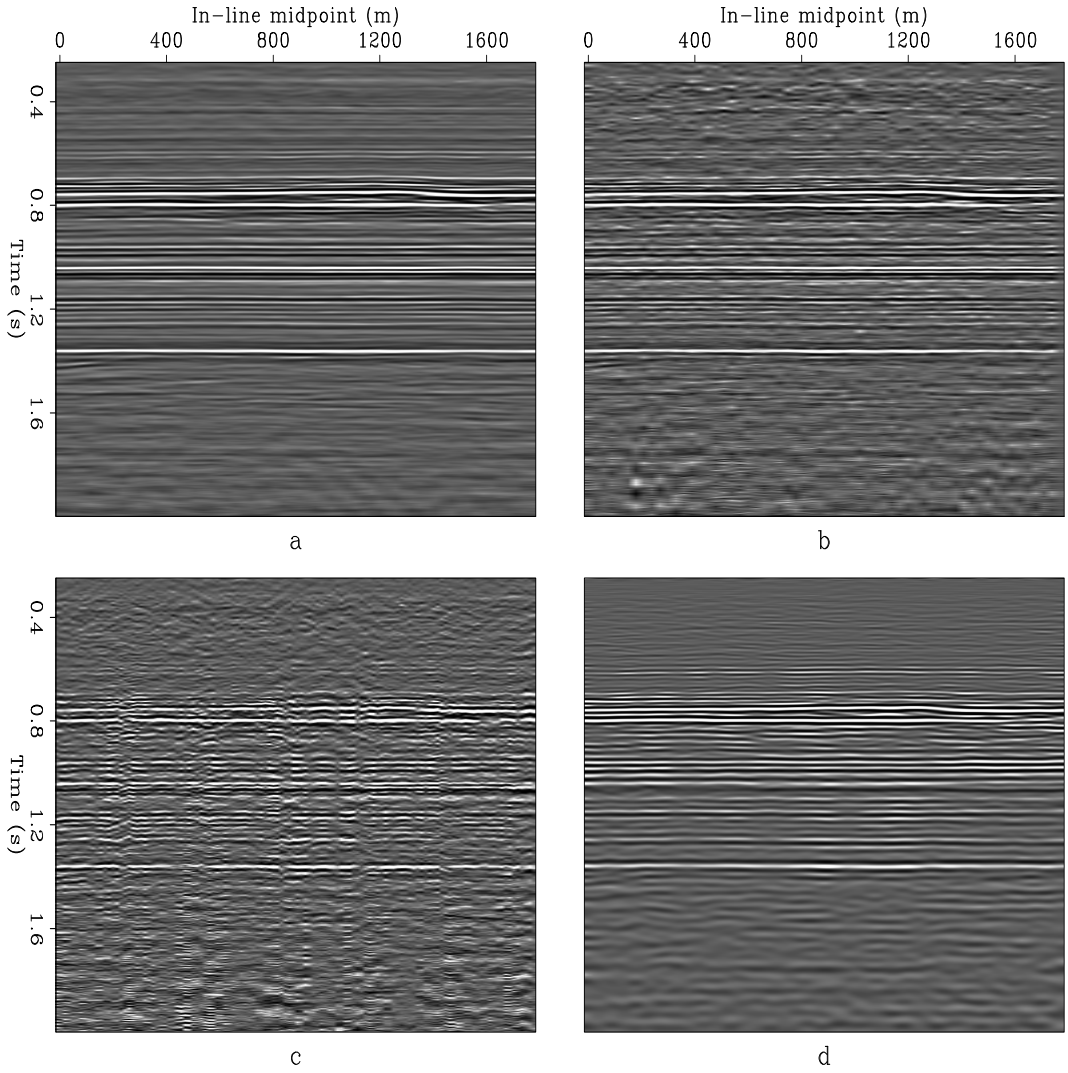

Figure 9.

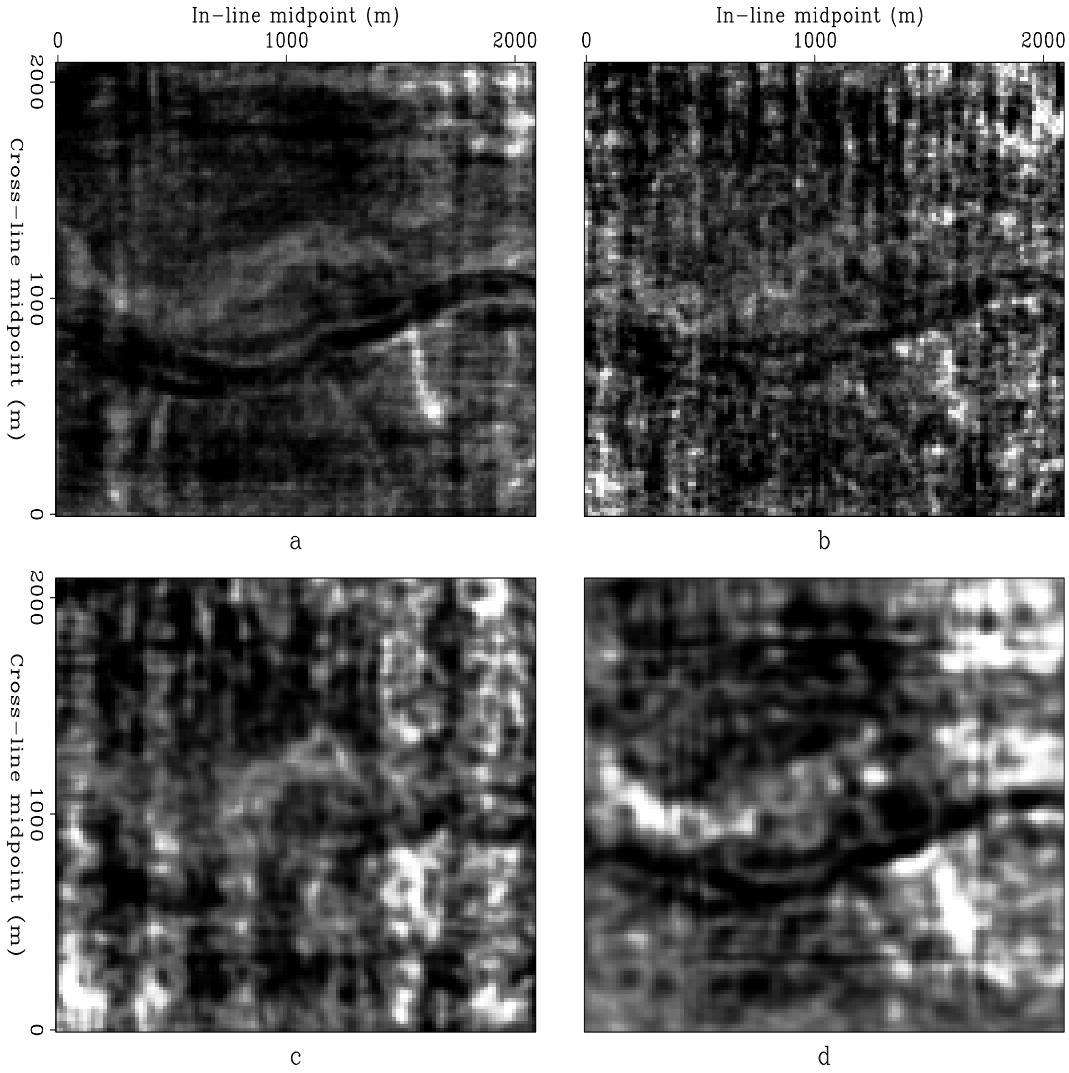
In−line midpoint (m)
0
1000
2000
Cross−line midpoint (m)
0
1000
2000
a
b
c
d

Figure 10.